Ionic liquids in the synthesis of nanoobjects

2010 Russ. Chem. Rev. 79 463

(http://iopscience.iop.org/0036-021X/79/6/R03)

Russian Chemical Reviews **79** (6) 463 – 477 (2010)

DOI 10.1070/RC2010v079n06ABEH004152

Ionic liquids in the synthesis of nanoobjects

N P Tarasova, Yu V Smetannikov, A A Zanin

Contents

I.	Introduction	463
II.	Synthesis of noble metal nanoparticles	464
III.	Synthesis of nanoparticles of metal oxides, chalcogenides and halides	468
IV.	Synthesis of nanoparticles based on non-metals	472
V.	Synthesis of nanocomposites	472
VI.	Synthesis of highly dispersed polymers	475

Abstract. The use of 'green' solvents, *i.e.*, ionic liquids, in the synthesis of nanoobjects or their stabilization is analyzed. The information is grouped according to the final products of syntheses, namely, noble metal nanoparticles, nanoparticles based on metalloids, nanoparticles of metal oxides, chalcogenides and nanocomposites and also fine-grain polymers. The shown data suggest that ionic liquids are among the key factors determining the structure and physicochemical properties of nanoobjects. The bibliography includes 82 references.

I. Introduction

In modern industry, the transition from the control over the emission and disposal of noxious substances and the destruction of hazardous wastes of chemical processes to fundamentally new methods of green chemistry becomes urgent. Green chemistry allows one not just to synthesize the desired substance but also to do this without inflicting any damage to the environment in all production stages. The use of green chemistry methods in industrial processes reduces the production costs because these methods involve no stages associated with the destruction or processing of hazardous side products, used solvents or other wastes. The reduction of the number of stages leads to energy saving, which also favourably affects the environmental and economic characteristics of the production.[1]

The problem of solvents in context of the general problem of transition to green chemistry turned out to be especially acute. The object was to carry out chemical processes solvent-free. However, in many cases this is impossible or unprofitable so far, hence it was necessary to find new solvents and propose new industrial processes that would comply with the definition of green chemistry, *viz.*, the design of chemical products and processes to reduce or to eliminate the use and generation of hazardous substances.[2] The solvents that meet these requirements include, in particular, ionic liquids.

Ionic liquids (ILs; low-temperature melts of organic salts) are viscous liquids that consist exclusively of ions and exhibit liophilic properties in a wide temperature range (the melting points fall in the temperature range from 233 K and, in certain cases, 183 K to 343 K). In this respect, they resemble ionic melts that can be prepared by heating common metal salts (*e.g.*, NaCl) to high temperatures. Organic ionic liquids are non-aqueous solvents.[3]

It is traditionally assumed that the first ionic liquid discovered was ethylammonium nitrate ($[EtNH_3]NO_3$; m.p. = 13 – 14 °C) obtained in 1914 by the famous chemist Walden and described in the *Proceedings of the Imperial Academy of Sciences* (St Petersburg).[4] Next reference to the 'ionic liquid' ('low-melting-point quaternary ammonium salt') was made only in 1934, when Grenacher[5] took out a patent for a new method of cellulose dissolution at temperatures below 100 °C. In 1951, Hurley and Wier[6] published a study of systems formed by *N*-ethylpyridinium bromide ([EtPy]Br) and metal chlorides (Fig. 1) at room temperature; however, they did not discuss the prospects of practical usage of such systems.

After the good solubilizing ability of ILs has been discovered, they came into use as the alternative to conventional solvents as well as in catalytic systems and electrochemistry. The advantage of ILs over the traditional highly volatile organic solvents is their low vapour pressure, which makes them fire-safe. Furthermore, due to their low volatility, they are less environmentally hazardous. The increased interest in the practical use of ionic liquids stimulated the appearance of ionic liquids with miscellaneous cations and anions in the market of chemicals, which,

N P Tarasova, Yu V Smetannikov, A A Zanin Institute of Chemistry and Problems of Sustainable Development, D I Mendeleev University of Chemical Technology of Russia, Miusskaya pl., 125047 Moscow, Russian Federation. Fax (7-499) 973 24 19, tel. (7-499) 973 24 19, e-mail: nptar@online.ru (N P Tarasova), tel. (7-499) 978 89 09, e-mail: smetyv@mail.ru (Yu V Smetannikov), tel. (7-499) 978 78 58, e-mail: alexey.zanin@gmail.com (A A Zanin)

Received 17 March 2010
Uspekhi Khimii **79** (6) 516 – 531 (2010); translated by T Ya Safonova

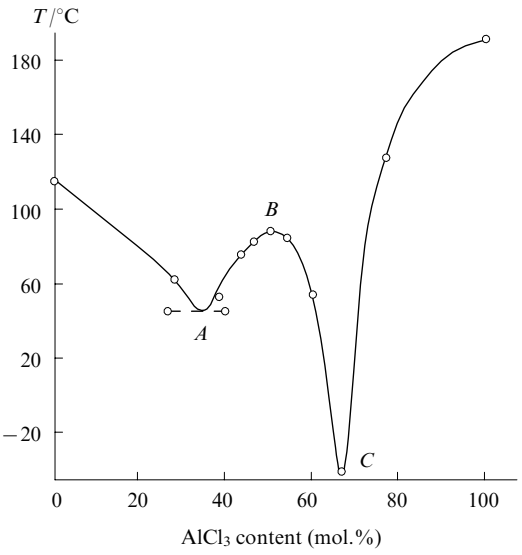

Figure 1. Phase diagram of the [EtPy]Br – $AlCl_3$ system.[6]
In points *A*, *B* and *C*, the [EtPy]Br : $AlCl_3$ ratio is 1 : 2, 1 : 1 and 2 : 1, respectively.

in turn, gave researchers the opportunity to 'tune' the IL properties to a particular task.

Depending on the cation, three basic types of ILs are recognized, namely, imidazolium $[RR'Im]^+$, pyrrolidinium $[RR'Pyr]^+$ and phosphonium $[R_3R'P]^+$ ionic liquids (R, R′ are alkyl groups, Im is the imidazolium cation, Pyr is the pyrrolidinium cation).[7] Table 1 shows their main physicochemical characteristics.[8–10]

Table 1. Main physicochemical characteristics of ionic liquids based on imidazolium, pyrrolidinium and phosphonium salts.

Ionic liquid [a]	M_{IL} /g mol^{-1}	ρ_{IL} /g cm^{-3}	η_{IL} /Pz	σ_{IL} /mS cm^{-1}
$[Bu^nMeIm]O_3SCF_3$	288.29	1.30	1.30	–
$[Bu^nMeIm]BF_4$	226.02	1.21	1.21	0.350
$[Bu^nMeIm]PF_6$	284.18	1.36	1.36	0.109
$[EtMeIm]N(SO_2CF_3)_2$	391.31	1.52	1.52	0.773
$[HxMeIm]N(SO_2CF_3)_2$	612.28	1.56	1.56	–
$[Bu^nMePyr]N(SO_2CF_3)_2$	422.41	1.40	1.40	–
$[Et_3OcP]N(SO_2CF_3)_2$	511.52	1.26	0.129	0.980
$[Et_3DdP]N(SO_2CF_3)_2$	576.63	1.21	0.180	0.470
$[Bu^n_3OcP]N(SO_2CF_3)_2$	595.68	1.18	0.250	0.268
$[Bu^n_3DdP]N(SO_2CF_3)_2$	651.79	1.13	0.303	0.177
$[Bu^n_3MeP]N(SO_2CF_3)_2$	497.50	1.28	0.207	0.416
$[Bu^n_3OcP]BF_4$	402.34	1.02	1.240	0.069
$[Bu^n_3DdP]BF_4$	458.45	0.97	1.310	0.047
$[Bu^n_3MeP]O_2PMe_2$	567.63	–	–	–

[a] Designations: Hx is hexyl, Oc is octyl, Dd is dodecyl.

At present, the best known stable ionic liquids are 1,3-dialkylimidazolium salts [RR′Im]X. The alkyl substituents R and R′ (for the most part, methyl or n-butyl groups) in the cation serve for 'tuning' the IL properties. The IL anionic part can be represented by various ions such as AlX_4^- (X = Cl, Br, I), PF_6^-, BF_4^-, $CF_3CO_2^-$, $CF_3SO_3^-$, $(CF_3SO_2)_2N^-$, *etc*.

Mixing of 1,3-dialkylimidazolium halide with an acid or a salt containing the chosen anion enables synthesis of ILs with the required set of properties, for example, $[Bu^nMeIm]^+AlCl_4^-$ is hygroscopic; $[Bu^nMeIm]^+PF_6^-$ is hydrophobic; $[Bu^nMeIm]^+OAc^-$ is water soluble. Virtually all ILs known are well characterized; the main approaches to tuning their physicochemical properties have been established.

According to contemporary concepts, 'pure' ILs based on imidazolium salts represent supramolecular polymeric structures with the high degree of self-organization. The IL structure involves three-dimensional networks of anions and cations bound by weak interactions (hydrogen bonds and intermolecular van der Waals forces).

Ionic liquids can be used together with organic solvents; it this case, as a result of solvation of the IL cations and anions, they are dispersed and, as a consequence, some of their physicochemical properties are changed, for instance, the viscosity decreases and the solution conductivity increases. By selecting ionic liquids, it was possible to extract the reaction products into another phase.[11] Being mixed with other solvents or metal nanoparticles, ILs formed nanostructured materials with polar and non-polar domains.

In the present review, an attempt was undertaken to summarize the experimental data on the use of ILs for the synthesis of nanoparticles (NP) or their stabilization.

II. Synthesis of noble metal nanoparticles

Metal nanoparticles can be prepared by chemical reduction of metal salts; thermal, photochemical or sonochemical decomposition of metal(0) complexes; hydrogenation of olefinic ligands of metal complexes; vapour phase deposition and electrochemical reduction of metals in high oxidation states. The formation of nanoparticles usually includes the following stages: 1) generation of atoms; 2) nucleation and formation of the initial atomic cluster; 3) growth of this cluster up to a certain size; 4) nanoparticle stabilization to prevent agglomeration. The general factor in the production of ultrafine systems is the presence of reagents that provide electrostatic or spatial stabilization of particles (Fig. 2).

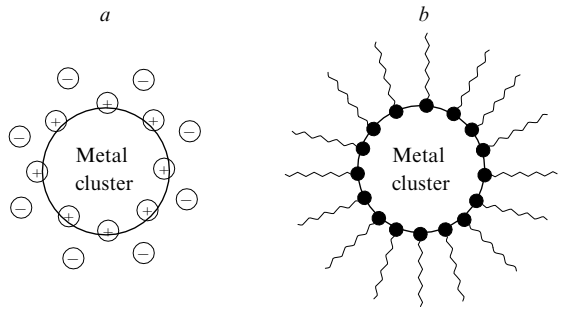

Figure 2. Mechanisms of stabilization of nanoparticles.[12]
(*a*) Electrostatic stabilization, (*b*) spatial stabilization.

The electrostatic stabilization of nanoparticles is based on formation of the electric double layer as the result of adsorption of ions of the same sign on the surface of the nanoparticle. Bulky counterions form the second layer that prevents the close approach of neighbouring nanoparticles and their agglomeration. The best known stabilizers include

cyclodextrins and polymers, for example, poly(vinylpyrrolidone), *etc*. The mechanism of stabilization of fine particles by large polymeric molecules with functional groups possessing high affinity to metal (thiol, sulfide, amino or phosphino groups) was studied in detail. Stabilizers of nanoparticles such as ionogenic surfactants, for instance, sodium dodecyl sulfate and dodecyltrimethylammonium chloride, also deserve mention. In 1996, Reetz *et al.*[13] showed that palladium NP (1.3–10.0 nm) stabilized with tetraalkylammonium salts are catalytically active in the Mizoroki–Heck reaction.

Srinivasan and co-workers[14] observed the formation of Pd nanoparticles upon the dissolution of palladium acetate in 1,3-dibutylimidazolium salts. Presumably, the growth of nanoparticles started with the formation of a heterocyclic carbene palladium complex. Chinese researchers[15] also observed the *in situ* formation of an N-heterocyclic carbene palladium complex by the Mizoroki–Heck reaction, which involved palladium acetate (the source of palladium) and 1-(n-butyl)-3-methylimidazolium bromide [Bu^{n}MeIm]Br (IL **1**). They assumed that nanosized palladium is the catalyst of the Mizoroki–Heck reaction. It was reported[16] that Pd nanoparticles were formed in a stereospecific reaction of alkene alkylation in IL in the presence of palladium acetate (the Mizoroki–Heck reaction),

It was found[17] that the reduction of the $Pt_2(dba)_3$ complex (dba is dibenzylideneacetone) dissolved in 1-(n-butyl)-3-methylimidazolium hexafluorophosphate [Bu^{n}MeIm]PF_6 (IL **2**) with molecular hydrogen (4 atm) at 75 °C afforded stable Pt(0) nanoparticles with the average size of 2.0–2.5 nm.

A detailed study of the behaviour and environment of Pt(0) nanoparticles in ionic liquid **2** suggested that the ionic liquid interacted with nanoparticles. The isolated Pt(0) nanoparticles could be redispersed in an ionic liquid or acetone or used in solvent-free hydrogenation of alkenes and arenes under relatively mild conditions (4 atm, 75 °C). Dispersed platinum nanoparticles could be reused in the hydrogenation reaction in an ionic liquid without substantial loss of their catalytic activity.

Imidazolium salts were also used[18] in the synthesis of catalytic systems based on Pd nanoparticles. The cation size determined by the size of the n-alkyl substituent had a considerable effect on the electrostatic stabilization, the size and the solubility of nanoparticles. At sufficiently high temperatures, imidazolium ionic liquids easily formed Pd complexes with heterocycle-derived carbenes due to deprotonation of the imidazolium salts. Such carbene-like ligands could be bound with surface palladium atoms of nanoparticles or form mononuclear biscarbene complexes.

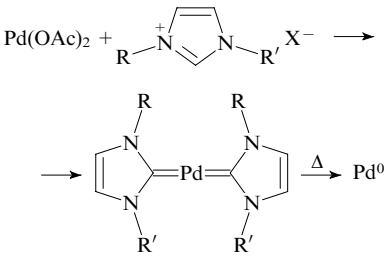

R = n-Alk, R′ = Me, Bu^n.

N-(3-Cyanopropyl)pyridinium salts react with $PdCl_2$ to form dinitrile complexes that were reduced with tributylphenylstannane to afford Pd nanoparticles. It was assumed that the nitrile group was weakly coordinated to the surface Pd atoms, and this was responsible for stabilization of nanoparticles.[19]

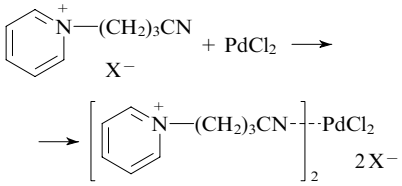

X = PF_6, BF_4, $N(SO_2CF_3)_2$; X = BF_4, PF_6, $N(SO_2CF_3)_2$.

Synthesis of Pt/Pd binary nanoparticles was described.[20] Metal compounds were dissolved in IL **2** and reduced with molecular hydrogen (4 bar, 348 K). Metal nanoparticles were isolated from solution by centrifugation. Studies of the structure of Pt/Pd particles by transmission electron microscopy (TEM) and X-ray diffraction analysis (XRD) has shown that the described processes afforded stable Pt/Pd particles (50% Pd and 50% Pt) and Pt particles with diameters of ~2.5 and ~4.0 nm, respectively.

Dispersed Ir(0) nanoparticles stabilized with trihexyl(tetradecyl)phosphonium methanesufonate [Hx_3TdP]O_3SMe (Td is tetradecyl) (IL **3**) were synthesized by reduction of the hydridoiridium carborane complex $(Ph_3P)_2Ir(H)(7,8\text{-}nido\text{-}C_2B_9H_{11})$ with hydrogen (10 bar, 160 °C).[21] The resulting iridium nanoparticles proved to be active catalysts in the arylborylation processes to afford boronic acids. The highest yield of products (91%) was achieved when the reaction was carried out in a microwave reactor in the presence of tetrakis(2-pyridyl)hydrazine as the base. Such a catalytic system could be used at least six times with the activity loss not exceeding 0.5%.

According to the published data, ionic liquids are very good stabilizers of transition metal nanoclusters; however, no clear explanation has been given to this phenomenon. An attempt was undertaken[22] to find experimentally the possible reasons for this phenomenon by the example of the synthesis of Ir(0) nanoclusters by reducing the iridium complex [(COD)Ir(MeCN)$_2$]BF_4 with molecular hydrogen in the presence of a proton sponge in acetone containing different amounts of the ionic liquid, 1-(n-butyl)-3-methylimidazolium bis(trifluoromethylsulfonyl)imide [Bu^{n}MeIm].$N(SO_2CF_3)_2$ (IL **4**).

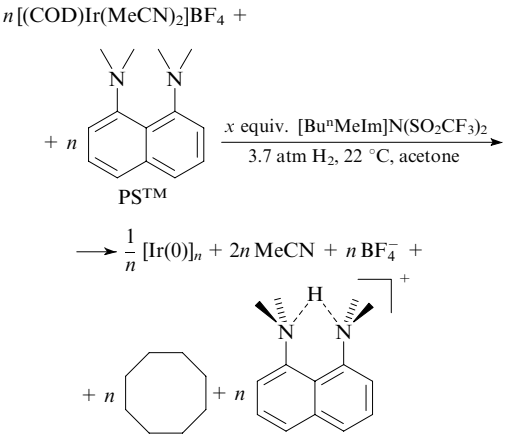

COD is cycloocta-1,5-diene, PS™ is the proton sponge.

In a control experiment in the absence of the ionic liquid, bulk metal was formed, whereas the addition of

10 equiv of IL **4** resulted in an Ir(0) nanocluster (2.1 ± 0.6 nm) (dark brown solution), which withstood agglomeration for 1 year. ^{2}H NMR studies have shown that the deuterium-labelled imidazolium cation of the IL reacted with the nanocluster surface to form carbene-like structures that stabilized the nanocluster. This was the first experimental confirmation for the stabilization of transition metal nanoparticles by ionic liquids.

Stable Ir(0) and Ru(0) nanoparticles measuring 2.0–2.5 nm were synthesized by the chemical reduction of their complexes in water-free IL **2**.[23]

The synthesis of well-dispersed Ru(0) nanoparticles stabilized by trihexyl(tetradecyl)phosphonium dodecylbenzenesulfonate (**5**) was described.[24] Ruthenium nanoparticles were prepared by the reduction of the $[(\eta^5\text{-}C_5H_5).Ru(\eta^5\text{-}C_5Me_5)Ru(\eta^5\text{-}C_5Me_5)]PF_6$ salt dissolved in ethylene glycol under a hydrogen atmosphere. The resulting red-brown solution was heated to 180 °C and kept at this temperature up to the change of its colour to black (for *ca.* 5 h) after which IL **5** was added and the solution was cooled to room temperature. After the removal of excess ethylene glycol in vacuum and washing the residue with a mixture of hexane and diethyl ether, a black sticky residue was obtained. The residue was dissolved in dichloromethane and subjected to centrifugation. The resulting ruthenium NP had the average size of 2.5 nm and a narrow size distribution. Ruthenium nanoparticles stabilized by ionic liquid **5** were stable in the argon atmosphere for more than a month.

Ru(0) nanoparticles catalyzed the isotope exchange between ^{10}B enriched diborane $B_{10}H_{14}$ and natural-abundance diborane:

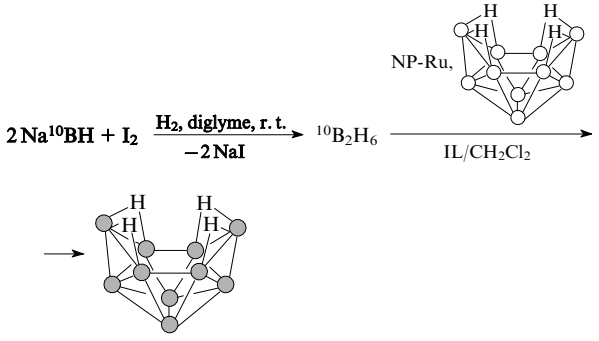

○ $^{11/10}$BH, ● ^{10}BH.

Ruthenium nanoparticles were also synthesized by the reduction of the $(COD)Ru(CH_2{=}CMe{=}CH_2)_2$ complex dispersed in the following imidazolium ionic liquids: $[Bu^nMeIm]N(SO_2CF_3)_2$, $[Bu^nMeIm]BF_4$, $[DcMeIm].N(SO_2CF_3)_2$ and $[DcMeIm]BF_4$ (Dc is decyl) with hydrogen (4 bar, 323 K).[25]

The size of nanoparticles was in the range of 2.1–3.5 nm. The finest nanoparticles were synthesized in the ILs that contained the weakest coordinating anion $N(SO_2CF_3)_2$. Ionic liquid-stabilized ruthenium nanoparticles were used in the reaction of biphasic hydrogenation of arenes. The catalyst-containing ionic liquid could be used many times without substantial loss of the catalyst activity.

It was noted that the size of 'soluble' metal NP was directly related to the self-assembling processes occurring in the ionic liquid and, hence, could be controlled by varying the reaction temperature, the length of alkyl substituents in the IL cation and the nature of the anion. Presumably,[25] the transition-metal nanoparticles in imidazolium ionic liquids are stabilized by either an oxide layer (if the latter was present of the metal surface), a protective layer of discrete supramolecules $\{[(RR'Im)_x(X)_{x-n}]^{n+}[(RR'Im)_{x-n}(X)_x]^{n-}\}$ (RR′Im is the dialkylimidazolium cation, X is the IL anion) through the loosely bound anionic groups, or N-heterocycle carbenes.

Table 2 shows the sizes of NP prepared in IL **4** by the reduction of the $(COD)Ru(CH_2{=}CMe{=}CH_2)_2$ complex with hydrogen (4 atm, 50 °C).

Table 2. Size of ruthenium nanoparticles prepared in the presence of ionic liquids.

Ionic liquid	Particle size before catalysis /nm	Particle size after catalysis /nm
$[Bu^nMeIm]N(SO_2CF_3)_2$	2.1 ± 0.5	2.8 ± 0.6
$[Bu^nMeIm]BF_4$	2.9 ± 0.5	3.3 ± 0.5
$[DcMeIm]BF_4$	2.7 ± 0.5	3.1 ± 0.5
$[DcMeIm]N(SO_2CF_3)_2$	2.1 ± 0.5	3.5 ± 0.5

In the majority of cases, ruthenium NP could not be isolated from IL solutions by centrifugation or the addition of solvents. However, for the colloidal suspension NP-Ru/$[Bu^nMeIm]BF_4$, the addition of acetone led to the separation of NP from the IL in 3–7 days. In contrast to Ru nanoparticles in the $[Bu^nMeIm]BF_4$ ionic liquid, colloidal suspensions of ruthenium nanoparticles in ionic liquids $[Bu^nMeIm]N(SO_2CF_3)_2$, $[DcMeIm]BF_4$ and $[DcMeIm].N(SO_2CF_3)_2$ were stable for weeks.

Rhodium nanoparticles (2.0–2.5 nm) stabilized with 2,2′-, 3,3′- or 4,4′-bipyridine (bipy) ligands were prepared by the reduction of $RhCl_3$ with sodium borohydride in different ILs.[26]

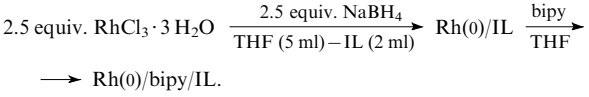

The authors of the above publication studied how the nature of a bipyridine ligand and the IL cations and anions affected the structure of the rhodium NP coordination sphere and noted that the IL in these systems served as both the solvent and the stabilizer.

Nanoparticles of Ir, Rh and Ru were synthesized in imidazolium {IL **2** or $[Bu^nMeIm]BF_4$ (**6**)}, *N*-(2-hydroxyethyl)-*N*-dodecyl-*N*,*N*-dimethylammonium, *N*-(n-butyl)-*N*-methylpyrrolidinium and 1-(n-butyl)-4-methylpyridinium ionic liquids.[26]

The reduction of original salts was instantaneous and accompanied by changes in the solution colour from red to black. The resulting suspensions of nanoparticles were stable for weeks. Rhodium nanoparticles were used in the catalytic hydrogenation of aromatic compounds. The selectivity of hydrogenation was found to depend on the nature of the bipyridine ligand. The highest selectivity was achieved with 3,3′- and 4,4′-bipyridines.

An interesting example of the effect of laser radiation on nanosystems was described.[27] It was found that the laser irradiation of relatively large Pd(0) and Rh(0) nanoparticles dispersed in IL **2** stimulated their fragmentation to finer particles with a narrow size distribution. The primary Rh and Pd nanoparticles were prepared from $PdCl_2$ and $[Rh(COD)(m\text{-}Cl)]_2$ dispersed in IL **2** by their reduction with molecular hydrogen (4 bar, 75 °C). In both cases, the

colloidal solution darkened. Nanoparticles of Pd(0) and Rh(0) dispersed in IL and subjected to laser irradiation proved to have irregular shapes and monomodal size distributions, namely, 4.2 ± 0.8 nm for Pd(0) and 7.2 ± 1.3 nm for Rh(0) (TEM data).

It is noteworthy that NPs separated from ILs could readily be re-dispersed under the action of laser radiation. The thus prepared colloidal solutions were stable for weeks. It was assumed that the ionic liquids perform different functions during the fragmentation. The plasmon absorption by metal nanoparticles is known to be sensitive to the nanoparticle environment. Ionic liquids could change the refractive index of the NP environment; moreover, ILs could form complexes with superficial metal atoms.

For the first time it was demonstrated [27] that the laser-induced excitation is an attractive method for the generation of stable metal colloids in ILs and regeneration of fine NP. For example, irradiation of Rh(0) nanoparticles stabilized with IL **2** led to a decrease in their size.

$$[Rh(0)]_n\,(\sim 15\text{ nm}) \xrightarrow[h\nu\,(532\text{ nm})]{\text{laser radiation}} [Rh(0)]_n\,(\sim 7\text{ nm}).$$

The formation of a porous silver film in a two-step process involving electrochemical formation of a binary silver–zinc alloy on a silver surface followed by electrochemical etching was described.[28] The single-bath deposition and dealloying steps were carried out in an ionic liquid $ZnCl_2$–1-ethyl-3-methylimidazolium chloride at temperatures below 150 °C without using other corrosive acids or bases. The temperature of the process was shown to affect the structure and the morphology of the porous silver film. The developed procedure allowed implementation of the process in a wide range of working temperatures and re-use of the ILs.

Stable silver nanoparticles were synthesized [29] by the hydrogen reduction of different inorganic salts AgX ($X^- = BF_4^-$, PF_6^-, $CF_3SO_3^-$) dissolved in the following ionic liquids: **6**, **2**, $[Bu^nMeIm]O_3SCF_3$ and $[Bu^nMe_3N].N(SO_2CF_3)_2$. The reactions were carried out in the presence of *N*-(n-butyl)imidazole as the scavenger of the side product (HX). The formation and stabilization of the silver NP in the hydrogen reduction of $AgBF_4$ can be depicted by the following scheme:

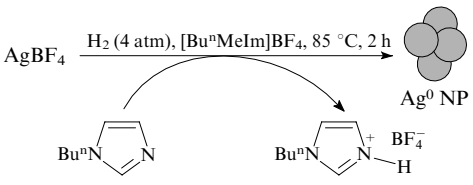

In the absence of *N*-(n-butyl)imidazole, the dispersion of nanoparticles in IL was unstable (the metal particles precititated within 1–2 h after the reduction). The size distribution of silver NP was very broad (in the range of several tens or even hundreds of nanometres). In the presence of *N*-(n-butyl)imidazole, the dispersion is stable (its lifetime under argon atmosphere is up to 3 days) and the size of nanoparticles ranges from 3 to 26 nm and the size distribution is uniform.

The thickness of the stabilizing layer around the silver NP was found to depend on the molecular volume of the IL anion; the latter also determined the range of sizes of silver nanoparticles. The physicochemical properties of ionic liquids such as density, viscosity, specific conductivity also correlated with the IL anion volume, although the contribution of supramolecular structures involving IL cations should be taken into account, too. Thus, the ionic liquids represent a fine tool for tuning the medium.

The synthesis of metal NP in aqueous solutions involved the use of 1-carboxymethyl-3-methylimidazolium chloride and 1-aminoethyl-3-methylimidazolium bromide as the stabilizer.[30] The size of the NP depended on the nature of the reductant. Thus smaller gold (below 3.5 nm) and platinum (below 2.5 nm) nanoparticles were prepared by the reduction with $NaBH_4$.

$$NaBH_4 + HAuCl_4 + H_2O \longrightarrow$$
$$\longrightarrow Au(0) + NaCl + H_3BO_3 + HCl + H_2,$$
$$NaBH_4 + H_2PtCl_6 + H_2O \longrightarrow$$
$$\longrightarrow Pt(0) + NaCl + H_3BO_3 + HCl + H_2.$$

The use of sodium citrate as the reductant led to larger gold nanoparticles (from 23 to 98 nm) with the particle size depending on the quantity of the reductant.

$$\begin{array}{l} \quad H_2C{-}COONa \\ HO{-}C{-}COONa + AuCl_4 \longrightarrow \\ \quad H_2C{-}COONa \end{array}$$
$$\longrightarrow Au(0) + CO_2 + NaCl + HCl + Me_2CO.$$

The morphology and the surface state of nanoparticles formed were characterized by transmission electron microscopy, UV-visible spectroscopy and X-ray photoelectron spectroscopy (XPS). In the X-ray photoelectron spectra of the metal NP surface, the C 1s and N 1s binding energies of ionic liquids were shifted negatively as compared with those of pure ionic liquids. It was found [30] that all metal NP can decorate the walls of carbon nanotubes. In this case, IL molecules served as the bridges that linked the metal NP to the carbon nanotube surface. Presumably, the positively charged imidazolium ring of the IL interacts with the π-electronic nanotube surface, while the functional groups in the side substituents (carboxy or amino groups) interact with the metal NP surface.

It was proposed [30] that the stabilization of gold nanoparticles can be (i) due to electrostatic interaction of the IL imidazolium cation with the negatively charged metal surface, (ii) due to coordination of the IL lateral functional groups to the metal atoms and (iii) due to the action of both factors.

A convenient sonochemical method for the preparation of gold NP stabilized with a thiol-functionalized IL, 1-[2,3-bis(mercaptoacetoxy)propyl]-3-methylimidazolium 3-mercaptopropane-1-sulfonate (**7**), was reported.[31] An aqueous solution of $HAuCl_4$ was added to a solution of IL **7** taken in different concentrations (Au : S molar ratios 2 : 1, 1 : 1, 1 : 2, 1 : 4 and 1 : 8); 30% hydrogen peroxide solution was used as the reducing agent. The size of the formed particles was found to depend on the Au : S ratio. Gold nanoparticles with the narrow uniform size distribution (2.7 ± 0.3 nm) were prepared at the molar ratio Au : S = 1 : 2 under sonication (40 kHz, 80 W) for 12 h (the reaction mixture changed its colour with the sonication time from light yellow to red). The red solution containing gold NP was stable for several weeks.

Gold NP were synthesized in the presence of an imidazolium IL containing a disulfide fragment.[32]

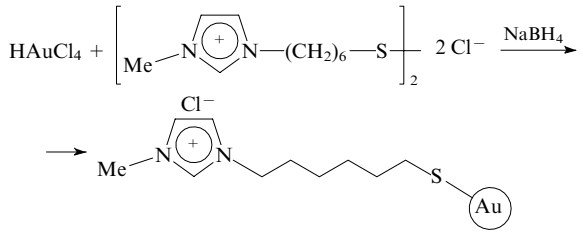

The formation of gold NP followed from the change in the solution colour from yellow to dark red. The hydrophilic and hydrophobic properties of IL-stabilized gold nanoparticles could be regulated by varying the IL cation. This was the first study devoted to the regulation of the surface properties of gold NP stabilized with imidazolium ionic liquids.

The average size of IL-modified gold nanoparticles was 5.0 nm. According to the results of thermogravimetric and elemental analyses, the stabilizer content in the gold NP was 10 mass %.

Closing this section, it should be noted that in addition to the above examples of the synthesis of metal nanoparticles in the presence of IL, information is available on the synthesis of Ir,[33] Ru,[34] Te,[35] Al,[36] Ag,[37] Pt [38] and Au [39] nanoparticles. Ionic liquids in these syntheses were used as the stabilizers and modifiers of the metal NP surface. It was found that functionalized ionic liquids (containing ester,[40,41] thiol [31,32,41,42] or carboxyl groups [30]) were found to much better stabilize aqueous suspensions of metal NP as compared with the ILs with cations devoid of functional groups.

All metal NP stabilized with ionic liquids interacted with the surface of crude (unprocessed) carbon nanotubes.

III. Synthesis of nanoparticles of metal oxides, chalcogenides and halides

Diverse methods are employed for the synthesis of IL-stabilized metal chalcogenides and oxides, namely, chemical co-deposition, sonochemistry, UV irradiation, *etc*. Recently, the high-frequency heating has received wide acceptance in the synthesis of nanoparticles. Microwave irradiation in combination with microwave-absorbing ionic liquids provided high heating rates, which accelerated and made easier the synthesis of such nanoparticles.

Microwave irradiation of a mixture of Bi_2O_3 (or Sb_2O_3), HCl, $Na_2S_2O_3$ and ethylene glycol (or ethanolamine) in the presence of ionic liquid **6** was successfully used in the synthesis of single crystal nanorods of Bi_2S_3 (or Sb_2S_3).[43] The ionic liquid was shown to have great effect on the morphology of M_2S_3 nanostructures (M = Bi, Sb). Thus in the presence of the IL, single-crystalline Sb_2S_3 nanorods were prepared, whereas in the absence of IL, single-crystalline nanosheets were synthesized. The products were characterized by XRD, TEM and electron diffraction methods.

Samples of Bi_2S_3 prepared by high-frequency heating at 190 °C in the absence of an ionic liquid had the structure of nanorods with diameter in the range of 50 – 100 nm and the length within 300 – 600 nm. In some cases, individual nanorods were formed.

The synthesis of Bi_2Se_3 nanosheets under microwave radiation was reported.[44] Selenium powder, solutions of $Bi(NO_3)_3 \cdot 5H_2O$ in ethylenediamine (EDA) or ethylene glycol (EG), HNO_3 and the ionic liquid $[Bu^nMeIm]BF_4$ were used as the starting reactants.

The morphologies of the nanoparticles formed are given in Table 3. As follows from these data, imidazolium ionic liquid **6** played an important role in the formation of Bi_2Se_3 nanosheets. In the absence of IL, when EDA was used as the solvent, nanoparticles and nanosheets were obtained, whereas in the presence of IL, irregular nanosheets were prepared. Presumably, the combined use of IL and microwave heating may also be useful in the synthesis of other binary nanostructures.

Table 3. Morphology of Bi_2Se_3 nanosheets formed under microwave radiation for different reaction systems.

Reaction system	T /°C	t /min	Morphology of nanoparticles
Se (0.01 g) + 5 M HNO_3 (sol., 0.5 ml) + + $Bi(NO_3)_3 \cdot 5H_2$ (0.041 g) + + EDAG (41.5 ml)	110	20	nanosheets and nanoparticles
Se (0.01 g) + 5 M HNO_3 (sol., 0.5 ml) + + $[Bu^nMeIm]BF_4$ (0.5 ml) + + $Bi(NO_3)_3 \cdot 5H_2$ (0.041 g) + + EDAG (41 ml)	110	20	irregular nanosheets
Se (0.01 g) + 5 M HNO_3 (sol., 0.5 ml) + + $Bi(NO_3)_3 \cdot 5H_2$ (0.041 g) + + EG (41.5 ml)	180	40	the same
Se (0.01 g) + 5 M HNO_3 (sol., 0.5 ml) + + $[Bu^nMeIm]BF_4$ (0.5 ml) + + $Bi(NO_3)_3 \cdot 5H_2$ (0.041 g) + EG (41 ml)	180	40	hexagonal nanosheets

Nanosized layered bismuthyl chloride (BiOCl) was synthesized [45] by a simple hydrothermal method from bismuth nitrate in the presence of 1-allyl-3-methylimidazolium chloride ([AllMeIm]Cl) by the following scheme:

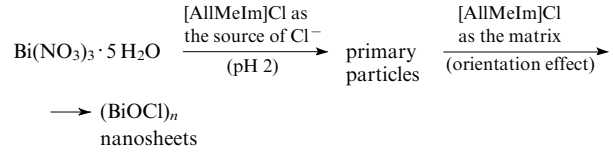

It was noted that the ionic liquid played a very important role in this synthesis serving as both the source of the Cl^- anions, as the reaction medium, as the organic dispersing agent and also as the nanoscale matrix.

The final product represented layered crystalline BiOCl nanoparticles with the tetragonal structure. The average thickness of NP was 55 – 70 nm.

The advantages of using ILs in synthesizing new materials and especially nanostructures has recently been demonstrated by the example of the synthesis of TiO_2 nanoparticles.[46 – 48] The nanoparticles synthesized in ionic liquids were spherical in place of the expected nanowires and nanorods. The advantages of ILs were better pronounced where the latter were used in combination with high-frequency heating, which was associated with the polarizability of IL anions.

Hydrolysis of titanium tetrachloride in hydrochloric acid in the presence of 1-ethyl-3-methylimidazolium bromide [EtMeIm]Br (IL **8**) produced nanoparticles of pure

rutile and the anatase–rutile composite.[48] It was shown that IL **8** plays the key role in the control over the structure and morphology of TiO_2 nanoparticles. The phase composition of products (the rutile-to-anatase ratio) depended on the bulk composition of the ionic liquid. Nanoparticles of TiO_2 with the desired phase composition were synthesized according to the scheme shown in Fig. 3.

The structural and morphological studies of synthesized samples have shown that anatase nanoparticles had the linear size within 4–6 nm and nanowires of pure rutile were 3–6 nm in diameter and 20–60 nm long.[48] It was found that $[EtMeIm]^+$ cations were capable of interacting with (110) rutile planes. First, the electrostatic interaction was possible between the $[EtMeIm]^+$ cation and the TiO_2 surface. It should be noted that at pH 3.5, the H^+ ions competed with the $[EtMeIm]^+$ ions for the electrostatic adsorption on the TiO_2 surface, where the former exhibited the higher electrostatic effect and acidity. However, the possibility to absorb on the TiO_2 surface was higher for the $[EtMeIm]^+$ ion, at least, in the second reaction step, because HCl and water gradually evaporated from the system. Second, besides the electrostatic interactions, other factors favoured the $[EtMeIm]^+$ interaction with the TiO_2 surface. Thus bulky $[EtMeIm]^+$ ions hindered the diffusion of H^+ cations to the TiO_2 surface; moreover, the interaction between the neighbouring imidazolium rings was present; finally, a hydrogen bond could be formed between the O atoms on the rutile surface and the H(C) atoms of the imidazolium ring. The interaction of rutile-bound imidazolium rings with one another made easier the formation of rod-like structures. Presumably, this method may serve as the commercial synthesis of metal oxide nanoparticles.

The synthesis of crystalline anatase (TiO_2) nanoparticles in ionic liquids has been carried out by several research groups. For instance, anatase nanocrystals of uniform shape with the narrow size distribution were synthesized by microwave heating of $TiCl_4$ in IL **8**.[48] It was reported that the adsorption configuration of the (101) anatase plane was close to that of the (110) rutile plane. The self-assembling ability due to the stacking interaction of the imidazolium cations depended on the length of the alkyl substituent in IL. Thus with the use of 1-(n-butyl)- (IL **1**) and 1-hexadecyl-3-methylimidazolium bromides (IL **9**) in the synthesis of TiO_2, pure rutile was prepared for the concentrations of ILs **1** and **9** equal to 0.1 and 0.05 mol litre^{-1}, respectively. The synthesized samples represented nanowires with the diameter of *ca.* 6 nm and the length of over 100 nm.

It was demonstrated for the first time that Ti nanowires can be also prepared by the electrochemical deposition from the $TiCl_4$–IL **4** ionic electrolyte.[49] The wire grown at constant potential for 20 min was characterized by the narrow size distribution (the diameter of 2 nm and the length of over 100 nm).

An interesting example of the possible practical use of TiO_2 nanocrystals prepared in the presence of IL was demonstrated.[50] The Gretzel cells (solar cells sensitized with dyes) with the mesoporous network of these nanocrystals were found to be highly efficient. Apparently, they

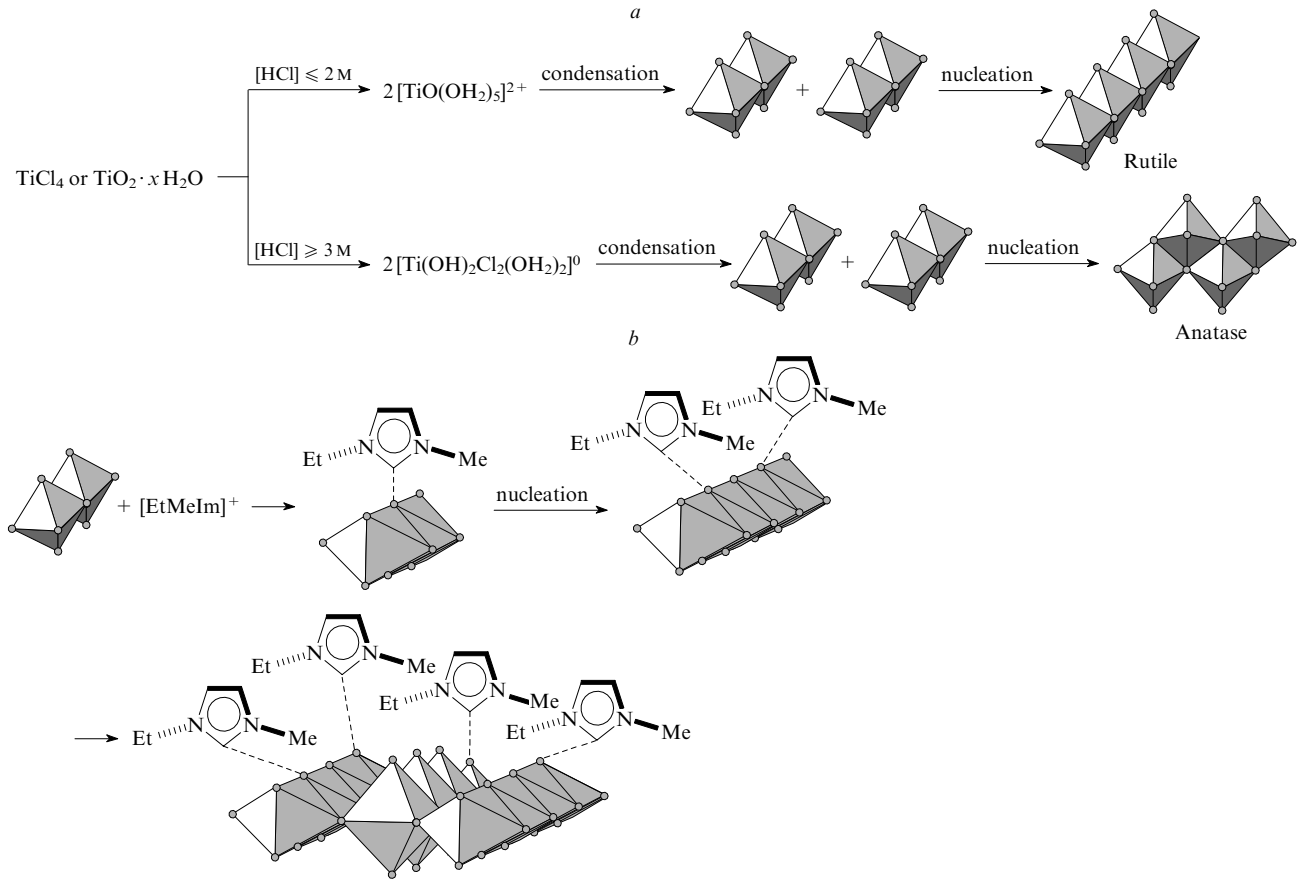

Figure 3. Illustration of the synthesis of TiO_2 nanocomposites with different rutile contents.[48] (*a*) In the absence of [EtMeIm]Br, (*b*) in the presence of [EtMeIm]Br.

Table 4. Samples of ZnO with different morphology synthesized in different ionic liquids.[51]

Ionic liquid	Run	Ratio $Zn(Ac)_2 \cdot 2H_2O$: NaOH	T /°C	Morphology	Average diameter /nm	Length /nm
$[EtMeIm]BF_4$	*1*	1 : 2	80	nanoparticles	10 – 20	
	2	1 : 4	80	nanorods	30 – 50	500 – 1500
	3	1 : 4	100	nanowire	30 – 40	1000 – 2000
	4	1 : 4	60	nanorods	50 – 80	500 – 800
$[Bu^nMeIm]BF_4$	*5*	1 : 2	80	nanoparticles	30 – 40	
	6	1 : 4	80	nanorods	100 – 200	200 – 600
$[Bu^nMe_2Im]BF_4$	*7*	1 : 2	80	nanoparticles	10 – 20	
	8	1 : 4	80		20 – 50	
	9	1 : 4	60		20 – 40	
	10	1 : 4	100		40 – 60	

can be a cheap substitute for inorganic photoelectric devices.

A simple low-temperature synthesis of ZnO nanostructures with the controlled shape in the presence of IL was reported.[51] The effect of IL cations on the shape of ZnO nanostructures and the mechanism of their formation was considered. Table 4 shows the obtained results.

The average size of all ZnO nanoparticles was *ca.* 10 – 20 nm, the ZnO nanowire had the diameter of ~ 30 – 50 nm and the length of 500 – 1500 nm. These studies allowed determination of the preferential orientation of the crystal growth axis.

The effect of the IL structure on the morphology of ZnO particles was followed by the example of samples synthesized in three different ILs under the same conditions (see Table 4, entries *2*, *6* and *8*).[51] The use of $[EtMeIm]BF_4$ led to ZnO nanorods with the length of *ca.* 500 – 1500 nm, whereas in the presence of $[Bu^nMeIm]BF_4$, nanorods of substantially smaller length (200 – 600 nm) were prepared. This suggests that the longer alkyl substutuents in position 1 of the imidazolium ring prevented the growth of 1D-ZnO. Nanorods became shorter due to spatial hindrance caused by long substituents. It deserves mentioning that in the presence of 1-(n-butyl)-2,3-dimethylimidazolium {$[Bu^nMe_2Im]BF_4$ (**10**)}, the morphology of the samples was completely different, namely, spherical nanoparticles formed. Apparently, hydrogen atoms in position 2 of the imidazolium ring determined the preferential growth direction of ZnO nanostructures. However, the lack of systematic data on the mechanism of formation of ZnO nanostructures in different ILs prevented the authors from drawing final conclusions. Thus it is known that the sample size depends on the rates of its nucleation and growth. The addition of an ionic liquid into the reaction system could lead, on the one hand, to inhibition of the particle agglomeration process; in this case, the process of molecular assembling proceeds at a low rate and the nucleation rate exceeds the growth rate. On the other hand, the peculiarities of the IL structure can stimulate the preferential growth of the crystalline ZnO nuclei in a definite direction that favours self-assembling of nanoparticles into desired nanostructures. Figure 4 shows the schematic diagram of growth of 1D ZnO nanostructures in an imidazolium ionic liquid.

Figure 5 illustrates the effect of the imidazolium cation structure on the formation of hydrogen bonds. Imidazolium cations are easily adsorbed on the surface of oxide nanoparticles containing the O_2^- cations due to electrostatic forces. The important role could be played also by hydrogen bonding between the hydrogen atoms in position 2 of the

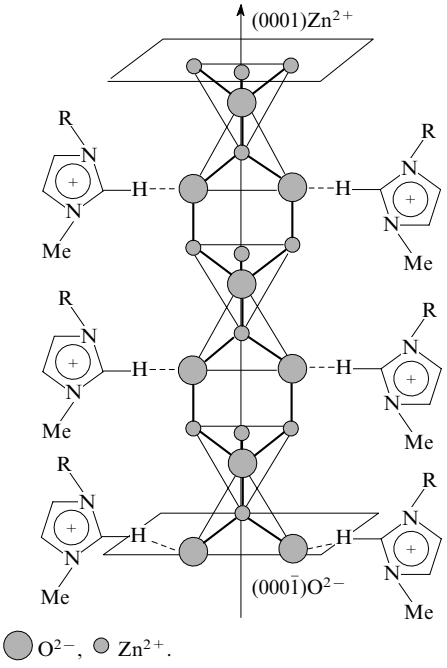

Figure 4. Illustration of the growth of ZnO 1D-nanostructures.[51]

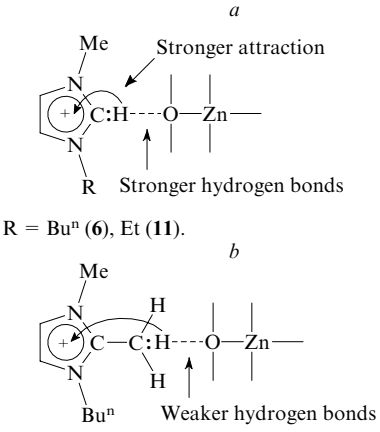

Figure 5. Formation of hydrogen bonds in IL **6**, **11** (*a*) and IL **10** (*b*).[51]

imidazolium ring and the oxygen atoms of the surface of ZnO nanoparticles. The hydrogen bonds formed between the $[EtMeIm]BF_4$ or $[Bu^nMeIm]BF_4$ ionic liquid and ZnO crystals were sufficiently strong.

When going from IL **6** to IL **10** where the methyl group is substituted for the hydrogen atom in position 2 of the imidazolium ring, the hydrogen bonding became less probable. The interaction of the imidazolium ring with the electron pair of the C–H bond became less strong, which weakened the hydrogen bond. The boning of the IL **10** cation with the ZnO nucleus weakened and the crystalline ZnO nuclei grew relatively freely. As the result, only ZnO nanoparticles were formed.

The effect of the reaction temperature on the morphology of ZnO nanostructures was also followed.[51] For the reaction carried out in $[EtMeIm]BF_4$ (IL **11**), the temperature rise from 60 to 80 °C changed the shape of ZnO samples from poorly pronounced ZnO nanorods to well pronounced nanorods. For higher temperatures (~100 °C), only ZnO nanowires were formed. This can be associated with the fact that the temperature increase favours the growth of longer structures. A finer effect of temperature on the morphology of nanostructures was observed for structures synthesized in IL **10**. Lowering the reaction temperature from 80 to 60 °C led to a decrease in the size of nanoparticles formed, while increasing the temperature from 80 to 100 °C resulted in the formation of coarser particles.

The hydrothermal (120 °C) synthesis of ZnO nanorods in IL **9** was reported.[52] The synthesized ZnO nanorods had the diameter of 80–200 nm and the length of several μm.

The supramolecular organization of lead bromides in imidazolium ionic liquids was described.[53] The synthesis of two crystalline imidazolium bromoplumbates, $[EtMeIm]PbBr_3$ (**12**) and $[Bu^nMeIm]_2PbBr_4$ (**13**), was carried out by heating 1-ethyl-3-methyl- and 1-(n-butyl)-3-methylimidazolium bromides with lead(II) nitrates under ionothermal conditions (in an autoclave under pressure). Both compounds had the extraordinary supramolecular organization with cylindrical channel formed by the dialkylimidazolium cations in which the bromoplumbate anions reside (Fig. 6 *a*,*b*).

Compound **12** was synthesized from IL **8**, cyclohexane-1,3-dicarboxylic acid and NaOH, while the synthesis of compound **13** involved the use of IL **1**, *meta*-phthalic acid and NaOH. It should be noted that in the absence of

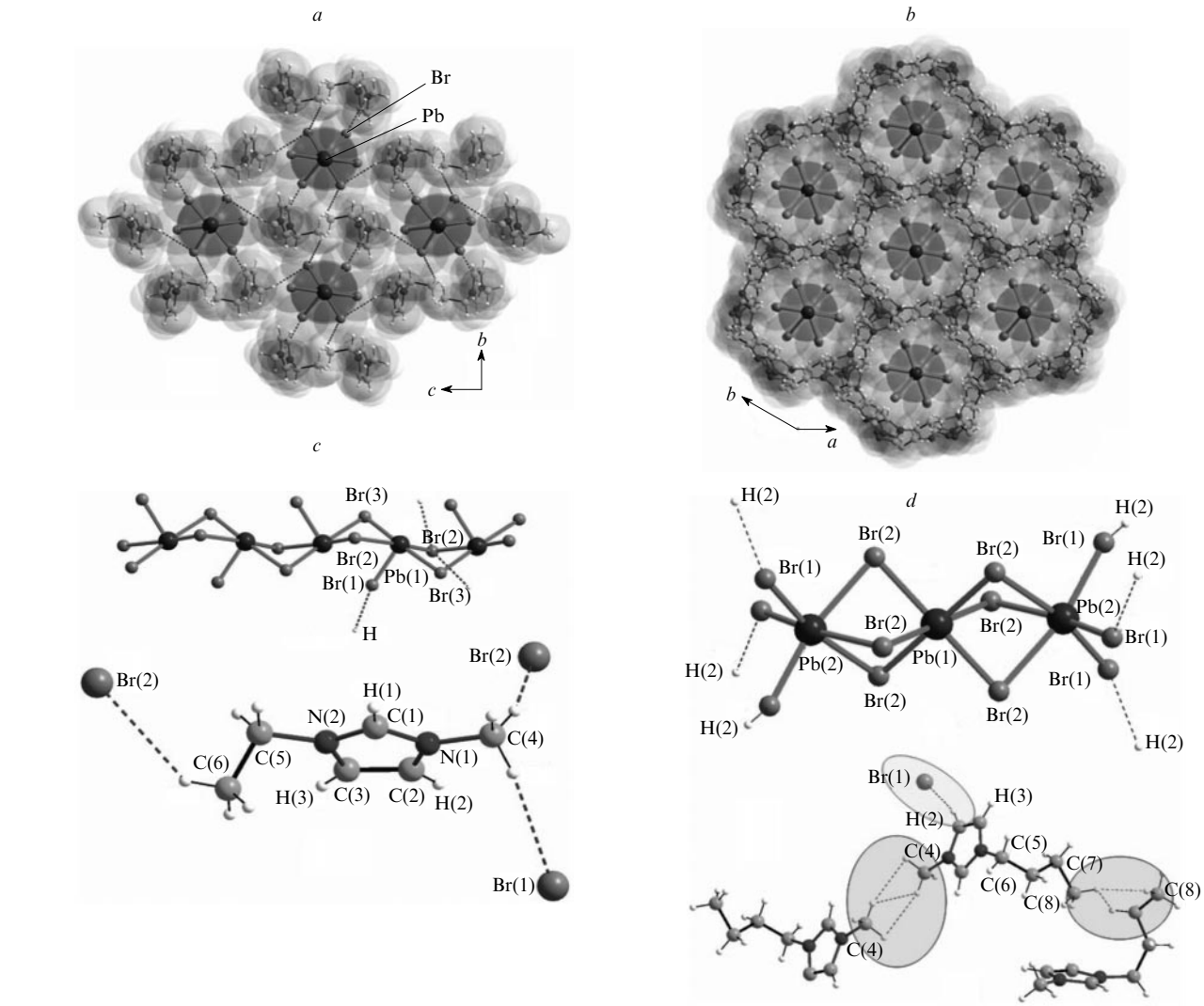

Figure 6. Supramolecular organization of lead(II) bromides in imidazolium liquids **8** (*a*) and **1** (*b*) and the structure of formed imidazolium bromoplumbates $[EtMeIm]PbBr_3$ (**12**, *c*) and $[Bu^nMeIm]_2PbBr_4$ (**13**, *d*).[53]

carboxylic acid or NaOH, the amorphous deposit or gel-like structures formed in place of crystalline products.

The unit cell of compound **12** contained the Pb^{2+} cation, the $[EtMeIm]^+$ cation and three Br^- anions. Each Pb^{2+} cation was surrounded by five Br^- atoms (hemidirected geometry). Polyhedra $PbBr_5$ were linked with one another to form 1D-chains $-Pb-Br-Pb-$. The imidazolium cation was bound to these chains by three weak hydrogen bonds $C-H\cdots Br$.

The unit cell of compound **13** contained two independent Pb^{2+}cations, one $[Bu^nMeIm]^+$ cation and two Br^- anions. One Pb^{2+}cation had the octahedral surrounding and the other had the tetragonal-bipyramidal surrounding of six Br^- anions (holodirected coordination geometry).

The $Pb(1)Br_6$ polyhedron was linked with two $Pb(2)Br_6$ polyhedra to form the linear Pb_3Br_{12} structure, which was bound with the $[Bu^nMeIm]^+$ cation by six weak $CH\cdots Br$ bonds. The imidazolium cations interacted with one another to form $CH\cdots C$ bonds.

The differences between channels in $[EtMeIm]PbBr_3$ (Fig. 6*c*) and $[Bu^nMeIm]_2PbBr_4$ structures (Fig. 6*d*) stemmed from the presence of a longer twisted alkyl chain (butyl substituent) in molecule **13** in the *gauche* conformation and the involvement of imidazolium-ring hydrogen atoms in the formation of hydrogen bonds $C(2)H\cdots Br(1)$ with the $PbBr_4$ anion.

IV. Synthesis of nanoparticles based on non-metals

A simple and convenient synthesis of selenium nanowires and microspheres by the chemical deposition at room temperature was developed.[54] Na_2SeO_3 and hydrazine hydrate were taken as the starting compounds. The deposition was carried out in the presence of 1,2,3-trimethylimidazolium tetrafluoroborate (IL **14**), or in the aqueous medium at 40 °C, or in the water–ethanol mixture at room temperature.

The products synthesized in different reaction mixtures had different shapes (Table 5).

Table 5. Synthetic conditions of different Se forms in IL **14** (2.3 mmol Na_2SeO_3 and 1.25 ml $N_2H_4\cdot H_2O$ as the starting reactants).

Reaction medium	Stirring	Morphology of Se nanoparticles
30 mmol $[Me_3Im]BF_4$ + + 10 ml H_2O + 50 ml EtOH	no	macrospheres (aggregates of nanorods)
30 mmol $[Me_3Im]BF_4$ + + 60 ml H_2O	"	club-shaped microspheres
30 mmol $[Me_3Im]BF_4$ + + 10 ml H_2O + 50 ml EtOH	yes	nanothreads and a few nanorods

In the first case, the formation of a large number of size-uniform microspheres (diameter 6 μm) that represented aggregated nanorods was observed. The reaction medium composition was assumed to be the only factor that determined the product morphology. It was also noted that ethanol acted as the catalyst in the redox reaction. Ethanol favoured the growth of one-dimensional Se nanoparticles and also the formation of microspheres and nanorods. The reaction carried out in the absence of IL **14** afforded no target product. Ionic liquid **14** played an important role in the formation of microspheres. In was assumed that this simple method would allow manufacture of other inorganic materials of controlled shape.

Nanocrystals of chalcogenides of different elements were synthesized by heating chalcogen (S, Se or Te) powders with $NaBH_4$ in imidazolium ionic liquids at 180–200 °C.[55] Nanorods and nanowires of Se and Te formed in IL **2** or **6** in the presence of poly(ethylene glycol) (PEG-600) as the co-solvent or without the latter. Nanowires of Se with incorporated dendrite structures were synthesized in the presence of PEG-600 and a small amount of water at room temperature, whereas sulfur microspheres were prepared by heating sulfur powder in a mixture of IL **6** and poly(ethylene glycol) at 150–250 °C. Under these conditions, crystalline nanostructures were successfully obtained.

The effect of the IL anion and the added surfactants on the size and shape of S, Se and Te nanostructures was studied [55] (Table 6).

Table 6. Nanostructures of S, Se and Te formed upon the action of $NaBH_4$ in ionic liquids **2** or **6** under different conditions.

Chalcogen	Reaction medium	Temperature /°C (time, h)	Morphology
S	IL **6** + PEG-600	180 (12)	microspheres of 18 μm diameter
Se	IL **2**	200 (10)	flower-like structures
	IL **2** + PEG-600	200	nanorods
	IL **6** + PEG-600 + + H_2O	75	lamellar structures
	IL **6** + PEG-600 + + H_2O	room temperature	nanowire (diameter ~150 nm, length 10 μm) + dendrite nanostructures (diameter ~100 nm)
Te	IL **2**	200 (10)	spherical microcrystals
	IL **2** + PEG-600	200 (10)	nanowires (diameter ~100 nm)
	IL **2** + trimethylcetylammonium bromide	200 (10)	nanorods (diameter ~100 nm, length 300–400 nm)

V. Synthesis of nanocomposites

The sol–gel synthesis of extremely well ordered monolythic superporous lamellar silica involved the use of several ionic liquids, particularly, 1-alkyl-3-methylimidazolium chloride, which served as the matrix in this method.[56]

Studies of the product structure have shown that the walls of the layered silica mesostructure are parallel to one another and contained pores with the diameter of 1.2–1.5 nm depending on the length of the alkyl substituent in the IL molecule. The results of atomic force and optical microscopy confirmed the extremely ordered lamellar phase structure of synthesized silica. The silica structure remained unchanged after the matrix was removed. The formation of this structure was explained by the formation of two-dimensional structures of IL molecules located between the neighbouring silica walls as the result of the spatial orientation of IL alkyl chains in parallel to the imidazole plane. Thus, a very unusual template of ordered lamellar supermicropores was formed. The temperature of the sol–gel

process had a great effect on the mesostructure of pores. Particularly, at 90 °C, the formation of worm-like structures was observed.

The synthesis of dispersions of silica nanoparticles used in the preparation of nanocomposite ionic gels was described.[57] The dispersion of silica nanoparticles in 1-ethyl-3-methylimidazolium bis(trifluoromethylsulfonyl)imide (IL **15**) was transformed into the gel even at a low silica concentration (2 mass % – 3 mass %), which was associated with the formation of a spatial network of silica in IL **15**. Dispersions of silica nanoparticles in IL were prepared by mechanical mixing followed by degassing to remove air bubbles from samples. Studies of the ionic conductivity and viscoelastic properties of formed nanocomposite ionic gels have shown that, although they behaved as solids, the nanocomposite gels exhibited the high ionic conductivity, approximately, 10^{-2} S cm^{-1} at 30 °C.

The possibility of synthesizing stable dispersions of silica particles both non-modified and modified with poly(methyl methacrylate) (PMMA) in different imidazolium ionic liquids such as IL **2**, **6** and 1-alkyl-3-methylimidazolium bis(trifluoromethylsulfonyl)imides was studied [58] (Fig. 7).

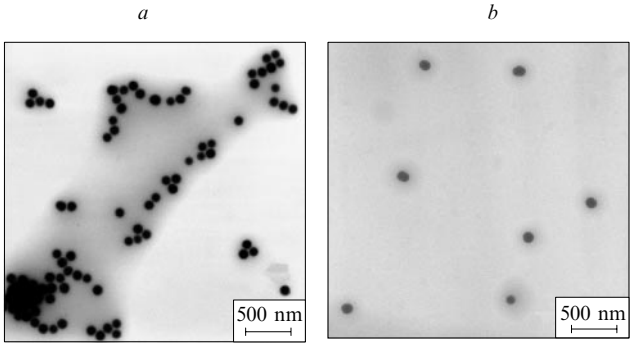

Figure 7. Dispersions of non-modified (*a*) and PMMA-modified (*b*) silica particles in ionic liquid [EtMeIm]N$(SO_2CF_3)_2$.[57]

According to theoretical estimates (using the equation of Deryagin – Landau – Verwey – Overbeek), non-modified silica particles cannot be stabilized and quickly aggregate in all ILs used in the above study (the instability of non-modified silica particles was confirmed experimentally). In contrast, the PMMA-modified silica particles formed stable dispersions in IL **2** and 1-alkyl-3-methylimidazolium bis(trifluoromethylsulfonyl)imides, but their dispersion in IL **6** proved to be unstable. This was attributed to the poor solubility of the grafted PMMA in this IL. Based on these observations, the importance of efficient spatial stabilization of silica nanoparticles in the synthesis of stable colloidal solutions was inferred.

The synthesis of nanostructured hybrid materials based on kaolinite by intercalating imidazolium ionic liquids into the interlayer space of kaolinite was described.[59] The following three ILs were used: 1-methyl-3-propylimidazolium bromide, 1-(2-chloroethyl)-3-methylimidazolium chloride and 1-benzyl-3-methylimidazolium chloride. Imidazolium salts were intercalated into kaolinite by a fine melt incorporation method using the dimethyl sulfoxide – kaolinite (DMSO-K) intercalate as the starting material (the IL : DMSO-K volume ratio was 4 : 1).

The structures, thermal behaviour and the compositions of nanostructured hybrid materials were characterized by several methods including X-ray diffraction, solid-state NMR, thermal gravimetric analysis and elemental analysis. The conductivity of synthesized materials measured at room temperature was 2×10^{-5} S s^{-1} and the maximum conductivity equal to 4×10^{-4} S s^{-1} was observed in a relatively short-range temperature interval of 160 – 200 °C. With the further increase in the temperature, the conductivity sharply decreased due to the decomposition of the organic material resulting in structural degradation. The structures of three nanostructured hybrid materials were optimized by using quantum chemical computations with a semi-empirical PM6 method. It was shown that bulky substituents in the imidazolium ring blocked the anion-active channels, which resulted in the decrease of conductivity.

A one-step sol – gel synthesis of antimicrobial Ag/TiO_2 nanocomposite powders containing silver nanoclusters was proposed.[60] By controlling the silver cluster size, it was possible to change the bactericide properties of such materials. The control over the size of Ag clusters was exerted by using IL. Ultrafine metal Ag nanoclusters were formed on the surface of TiO_2 (anatase) nanoparticles after the gel calcination. The ionic liquid used was IL **2**; $AgNO_3$ and $Ti(OPr^i)_4$ served as the sources of the Ag atoms and TiO_2 particles.

The antibacterial tests of samples prepared with IL **2** and containing 3.9 mass % and 7.4 mass % Ag/TiO_2 have shown that the bacterial growth slowed down by 99.9% and 98.8% for the Ag concentrations of 1.6 and 1.2 μg ml^{-1}, respectively.[60] Complete inhibition was reached for the Ag content of 2.4 μg ml^{-1}. Such a difference in the inhibition was explained by the different sizes of Ag clusters adsorbed on the surface of TiO_2 particles. Presumably, for the high inhibitory activity, the average size of Ag clusters should be less than 5 nm with the simultaneously high Ag content (7.4 mass %) in the composite. As the reference samples, TiO_2 powder and an Ag/TiO_2 sample (5 mass % Ag) synthesized in the absence of IL, both exhibiting weak antibacterial properties under these conditions, were taken.

Studies [61 – 63] were devoted to the surface functionalization of single-walled carbon nanotubes (SWNT) with different organic derivatives in the presence of ionic liquids. The tubes were functionalized [61] with aryldiazonium salts at room temperature in the presence of an IL and K_2CO_3 (Fig. 8). The authors characterized their method as a 'pestle-and-mortar method of nanotube functionalization in ionic liquids' and noted its quickness and safety. They used miscellaneous ILs under different conditions. The resulting products were characterized by advanced physicochemical methods.

It was demonstrated that non-covalent donor-acceptor complexes can be synthesized from easily accessible sapphirine diol ('extended' porphyrin) and SWNT in the aqueous medium and in ionic liquid **2**.[62] It was noted that this ionic liquid is one of the most efficient for exfoliation (surface peeling) of nanotubes. In the synthesis of supramolecular complexes in the aqueous medium, purified SWNT were pre-sonicated, whereas in IL, nanotubes were simply ground with a pestle in a mortar.

Spectral studies and the data of electron microscopy have shown that sapphirine-modified carbon nanotubes were capable of transmitting photoexcitation by the electron transfer mechanism and, hence, capable of light absorption.

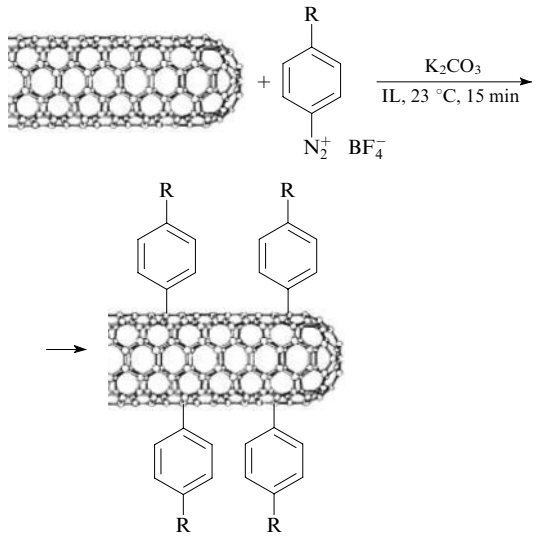

Figure 8. Functionalization of single-walled carbon nanotubes with aryldiazonium salts in the presence of IL and K_2CO_3.[61]

A method of electrochemical modification of SWNT with *N*-succinimidyl acrylate (**16**) in the presence of IL **2** was proposed.[63] For this purpose, SWNT were mixed with IL **2** up to the gel formation followed by the addition of modifier **16** after which the gel was transferred to a cell with a conducting substrate such as gold. After the electrochemical treatment involving grafting of acrylate **16** onto the SWNT surface, the resulting samples were extracted from IL **2**, washed, centrifuged, sonicated in acetone and then dried in vacuum. It was stressed that this method allows functionalization of SWNT in large quantities.

The advantages of using fluorinated ionic liquids for accelerating the growth of semiconductor InP and CdSe nanocrystals under microwave radiation were demonstrated.[64] The InP crystals were characterized by a low quantum yield of photoluminescence (< 4%), which was explained by the presence of phosphorus atom vacancies in this material. The treatment of the InP surface with hydrogen fluoride (etching) resulted in the removal of phosphorus vacancies from the crystal surface and increased the quantum yield to 38%. However, the high quantum yield (47%) of InP nanocrystals could be achieved without the HF treatment, by combining the microwave treatment with the addition of an IL containing a fluorinated anion.[65] The growth of InP nanocrystals in the presence of an ionic liquid such as 1-hexyl-3-methylimidazolium tetrafluoroborate occurred simultaneously with the surface etching. The optimization of this process was achieved by varying the rates of growth and etching.

The properties of InP nanocrystals depended on both the nature of the IL anions (BF_4^-, PF_6^- or Cl^-) and the IL concentration. For samples grown for the molar ratio In : IL = 1 : 10, the quantum yield tended to decrease in the following series:

$$BF_4^- > PF_6^- > Cl^-,$$

whereas for samples grown for the 1 : 1 ratio, the following series was observed:

$$PF_6^- > BF_4^- > Cl^-.$$

The observed IL-concentration-dependent change in the anion effect reflected the number of formed F^- ions. It should be noted that PF_6^- has a stronger ability to form fluoride ions as compared with BF_4^-.

Synthesis of boron nitride layers by the ionothermal method in the presence of IL **10** was described,[65] where KBH_4, $NaNH_2$, Li_3N and IL **10** were used as the starting compounds. In this synthesis, IL **10** simultaneously performed several functions, namely, it served as the source of the boron atoms, the solvent and the matrix. The obtained samples were characterized by XRD, XPS, FTIR spectroscopy and TEM. The results of studies pointed to the involvement of hydrogen bonds in the formation of BN nanolayers.

Ionic liquid **10** exhibiting high ionic conductivity was assumed to favour the fast transfer of electrons from KBH_4 to $NaNH_2$; moreover, it provided the high ionic strength of the reaction system, which improved the reagent solubility and increased the reaction rate. It deserves mention that ionic liquids, like water, exhibit polar properties but in contrast to water have low surface tension.

The synthesis of Ta adhesion layers in TaF_5-containing 1-(n-butyl)-1-methylpyrrolidinium bis(trifluoromethylsulfonyl)imide (IL **17**) was described.[66] In the same study, the possibility of synthesizing nano- and microcrystalline aluminium in ionic liquids was mentioned. Nano- and microcrystalline aluminium was electrochemically deposited in three air- and water-stable ionic liquids, namely, ILs **15**, **17** and $[Hx_3TdP]N(SO_2CF_3)_2$. It was found that with the addition of $AlCl_3$ to ionic liquids **15** and **17**, the solution was separated into layers to form biphasic systems for the $AlCl_3$ concentrations in the range from 2.5 to 6.0 mol litre^{-1} (for IL **15**) and 1.6 to 2.5 mol litre^{-1} (for IL **17**). The electrodeposition of aluminium from ionic liquids **15** and **17** at room temperature occurred only from the upper phase for the $AlCl_3$ concentration $\geqslant 5$ and $\geqslant 1.6$ mol litre^{-1}, respectively. Aluminium layers characterized by high adhesion were electrodeposited onto the surface of low-carbon steel by using $AlCl_3$-containing IL **15**. In the same study,[66] the synthesis of 100-nm thick layers of elemental silicon by its deposition onto gold particles in IL **17** was described, $SiCl_4$ was used as the silicon source.

Remarkable catalysts were synthesized by immobilization of 1,1′-bis(diphenylphosphino)ferrocenepalladium trifluoroacetate {[Pd(dppf)]$(CF_3CO_2)_2$} and imidazolium salts of trifluoromethanesulfonic acid on the silica surface.[67] As the IL, four imidazolium salts with the polarity decreasing in the following sequence were used:

$$[EtMeIm]^+ > [Bu^nMeIm]^+ > [HxMeIm]^+ > [HxMe_2Im]^+.$$

This study also provided experimental data that confirmed the formation of spatial palladium structures in a thin superficial IL film.

It was shown that the adsorption of IL molecules on the silica surface was accompanied by the decrease in the fluidity of imidazolium cations. Samples prepared by dissolving [Pd(dppf)]$(CF_3CO_2)_2$ and CF_3SO_3H in original IL exhibited higher viscosity as compared with the original IL.

It was reported[68] that the surface of metal NP can be modified with 1-methyl-3-[3-(trimethoxysilyl)propyl]imidazolium chloride (IL **18**) to impart them valuable properties. Thus as the result of modification with IL **18**, the hydrophilic gold NP acquired hydrophobicity after their treatment with an aqueous HPF_6 solution. Non-modified iron oxide nanoparticles, which were used as the contrast sub-

stances in magnetic-resonance imaging for diagnosing liver diseases, after the modification with IL **18** could be used in diagnosing diseases of other organs. Attention was focused on the fact that this was the first example of the *in vivo* use of IL. Modified iron oxide NP were synthesized according to the scheme shown in Fig. 9.

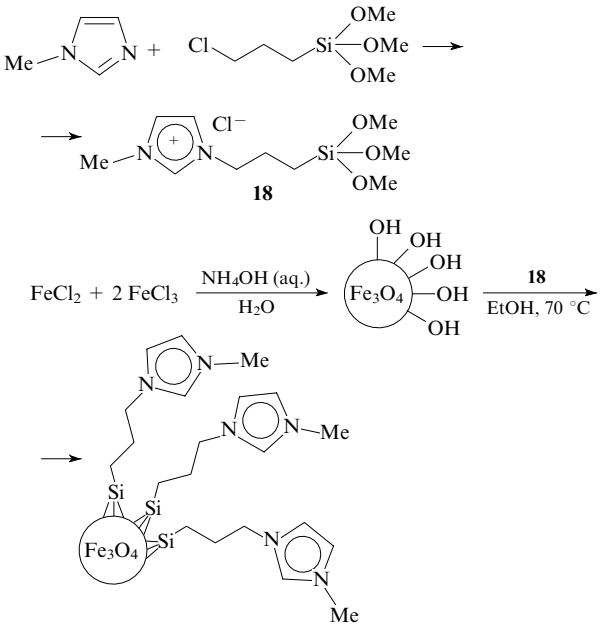

Figure 9. Scheme of synthesis of modified Fe_3O_4 composites.[68]

Addition of 0.5 M aqueous solution of potassium bis(trifluoromethylsulfonyl)imide to the aqueous dispersion of Fe_3O_4 nanoparticles in IL **18** led to immediate deposition of iron nanoparticles. The anion was removed by washing with 1 M NaCl solution. The toxicity of the NP-Fe_3O_4/IL **18** product was assessed both *in vitro* and *in vivo*. The studies revealed no considerable difference between the toxicological characteristics of NP-Fe_3O_4/IL **18** and the contrast substance Resovist®. Attention was drawn to yet another potentially promising application field of modified iron oxide nanoparticles. They can be used as the matrices for DNA sequencing.

A similar approach was used[69] in modifying the iron oxide properties aimed at the production of hybrid materials.

VI. Synthesis of highly dispersed polymers

In a series of studies,[70–75] the possibility of synthesizing highly dispersed polymeric forms of phosphorus (modified red phosphorus) with desired properties was considered.

Studying the radiation-induced polymerization of white phosphorus (WP) in non-polar media (benzene, haloalkanes, hexane), it was shown[70] that such processes afford highly dispersed phosphorus-containing polymers with micron grains that exhibited several useful properties (high thermal stability, low phosphine release, *etc.*)

It was found[71] that after the introduction of ionic liquid **15** into the WP–DMSO and WP–benzene–DMSO mixtures, the 100% conversion with respect to white phosphorus was achieved even for the absorbed doze of 20 kGy. The observed increase in the phosphorus polymerization rate in the presence of IL was probably due to the formation' of the [P_4–IL] complex.[72] It was demonstrated that the optimal reaction system for the WP polymerization is the benzene–DMSO–IL system in which the structuring of reaction mixture components occurs, which leads to their aggregation to nanostructures.

The effect of the ionic liquid structure on the kinetics of WP polymerization was studied. For the $[Bu^nMeIm]^+X^-$ ($X^- = BF_4^-$, PF_6^- and $CF_3SO_3^-$) ionic liquids, in the range of ratios $[IL]_0 : [P_4]_0 = 0–45$, with the $BF_4^- \rightarrow PF_6^- \rightarrow CF_3SO_3^-$ transition, the maximum of effective constants was observed to shift to higher IL contents, *i.e.*, the widest change in the effective constant was observed for $[Bu^nMeIm]O_3SCF_3$. The observed dependences of effective constants on the $[IL]_0 : [P_4]_0$ ratio for ILs containing different cations but the same anion suggested that the IL cationic part was also involved in the process.

Imidazolium and phosphonium ILs favoured the formation of nanosized particles of polymeric phosphorus, affected the product composition and enhanced the degree of conversion and the radiation-chemical yield of phosphorus-containing polymers.[74,75]

It was shown[73] that P_4 molecules behaved in polymerization reactions in the same manner as olefins; hence, one can be expect the aforementioned relationships to be also typical of the polymerization of various olefins in the presence of ILs.

It was shown[76] that four amphiphilic diblock co-polymers of poly(buta-1,2-diene) with poly(ethylene oxide) (PB–PEO) with different content of poly(ethylene oxide) aggregated in IL **2** to form micelles. Depending on the conditions and the diblock co-polymer composition, different micellar structures could be obtained, namely, spherical micelles, worm-like micelles and bilayer bubbles. Micellar nanostructures were directly observed using cryogenic TEM and dynamic light scattering. Solutions of diblock co-polymers PB–PEO in IL **2** as compared with aqueous solutions of the same co-polymers exhibited certain peculiarities, for instance, the micelle morphology was independent of the temperature in the range of 25–100 °C.

The stability of lyotropic liquid crystals of non-ionogenic surface-active alkyl ethers of poly(ethylene oxide) C_nE_m with alkyl chains of different length, formed in ethylammonium nitrate (IL **19**), was studied.[77] It was noted that the processes of self-assembling of the liquid crystal mesophase in IL **19** were completely analogous to those observed in water. The only quantitative difference of the C_nE_m self-assembling in IL from their self-assembling in water was that the formation of the liquid-crystal mesophase in ethylammonium nitrate required the presence of longer alkyl chains in ether molecules. Long alkyl chains favoured the C_nE_m self-assembling in ammonium nitrate to form bulky 'solvophobic' structures.

Microemulsions formed in the system IL **6**–cyclohexane– surfactant Triton X-100 were studied.[78] This system proved to be analogous to water–oil microemulsions. The neutron scattering data pointed to the presence of IL nanodrops dispersed in cyclohexane. The data on polymerization of microemultions containing IL **6** (30 mass %), styrene (47 mass %) and a surfactant [1-(2-methylacryloyloxyundecyl)-3-methylimidazolium bromide (23 mass %)] were also shown. As the result of polymerization, the IL **6**/polystyrene composite membranes were obtained and their structure was characterized by different methods. A

membrane containing 5 mass % IL **6** represented a 'continuous' polystyrene matrix with incorporated IL **6** droplets with the diameter ~20 nm. A membrane containing 30 mass % IL **6** consisted of individual polystyrene domains measuring 15–25 nm and long through channels of IL molecules (measuring 15–25 nm). It deserves mentioning that the size of certain channels (IL domains) at their bases coincided with the size of inner pores (~10 nm).

The aggregation of a fluorinated cationic surfactant FC-4 in IL **2** and **6** was studied.[79] It was shown that the surface activity of FC-4 in ionic liquids was higher as compared with other conventional surfactants. The analysis of the temperature dependence of surface tension has shown that the formation of FC-4 aggregates in IL **6** at temperatures above 30 °C was governed by enthalpy the same as for surfactant micelles in aqueous solutions. Thermodynamic and ^{1}H NMR spectroscopic studies have shown that FC-4 molecules in IL **6** formed micelles, whereas in IL **2** they formed nanodrops. The formation of micelles in IL **6** was associated with solvophobic interactions between the chains of FC-4 molecules (like the hydrophobic interactions in an aqueous solution). Studying self-assembling processes for FC-4 in ionic liquids with different hydrophilicity makes it possible to gain insight into the self-assembling mechanism of surfactants in different ionic liquids.

Several studies (*e.g.*, see Refs 80–82) were devoted to the use of ILs in classical polymerization processes. Thus it was reported[80] that IL **2** was used as the medium in the synthesis of poly(methyl methacrylate) NP by the polymerization reaction. An electrochemical synthesis of tubular polyaniline structures in IL **2** containing 1 mol litre^{-1} of trifluoroacetic acid was described.[81] Nanotubes were deposited onto modified glass at room temperature. Tubular polyaniline structures with the diameter of 120 nm were studied by scanning electron microscopy. Polyaniline formed in IL was found to be electrically conducting. Varying ILs made it possible to control the polyaniline conductivity. An interesting example of the synthesis of nanostructured conducting polymeric materials, namely, polypyrrole and poly(*N*-methylpyrrole), in magnetic 1-(n-butyl)-3-methylimidazolium tetrachloroferrate (IL **20**) was described.[82] Presumably, the proposed synthetic method allows different nanosized conducting polymer materials to be prepared by the simple assembling of monomers in IL **20**. In this synthetic method, IL **20** simultaneously acted as the catalyst, the dopant and the solvent.

Synthesized at room temperature, polypyrrole NP had the size of 50–100 nm and represented almost regular spheres. As the temperature increased, coarser NP were obtained (approximately 700 nm at 80 °C). Varying the reagent concentration and the polymerization time had no effect on the characteristics of polymeric forms. Presumably, in this case, IL **20** solutions acted as the liquid phase matrix. It is noteworthy that the self-organized nanostructures (spherical particles) of the conducting polymer were formed in the absence of magnetic field. In the presence of magnetic field, nanotubes were formed. It was noted that this was the first synthesis of nanotubes by an assembling process. It was shown that polypyrrole NP can be aligned along the external magnetic field lines. Thus, the external magnetic field exerted influence on these local structures and, hence, on the final structure of the polymer. It was inferred that magnetic ionic liquids are the new promising solvents for synthesizing π-electron conjugated polymers.

* * *

The data presented in this review illustrated the widely diverse potentialities of ionic liquids in synthesizing nanoobjects of the different physicochemical nature. Virtually all ILs known are well characterized. Their low toxicity, high dissolving ability, high thermal and radiation stability and other characteristics make it possible to assign them to green solvents. The market of commercially accessible ILs is constantly extending.

The possibility of tuning the IL structure and physicochemical properties to the synthesis of particular nanoobjects allows the IL application fields to be widened. However, it should be noted that the studies on the synthesis of nanoobjects with the use of ILs are still in the stage of primary data collecting and make it possible to draw only preliminary prognoses on the effect of the nature and structure of ILs on the mechanism of formation and stabilization of nanostructures.

References

1. V V Lunin, E S Lokteva *Zelenaya Khimiya v Rossii* (Green Chemistry in Russia) (Eds V V Lunin, P Tundo, E S Lokteva) (Moscow: Moscow State University, 2004)
2. P T Anastas, in *Clean Solvents, Alternative Media for Chemical Reactions and Processing (ACS Symp. Ser.)* Vol. 819 (Eds M A Abraham, L Moens) (Washington, DC: American Chemical Society, 2002) p. 1
3. M Koel, K Mihkel *Proc. Estonian Acad. Sci. Chem.* **49** 145 (2000)
4. P Walden *Bull. Acad. Impgr. Sci.* **8** 405 (1914)
5. US P. 1943176 (1934)
6. F H Hurley, T P Wier *J. Electrochem. Soc.* **98** 207 (1951)
7. T Welton *Chem. Rev.* **99** 2071 (1999)
8. K Tsunashima, M Sugiya *Electrochem. Commun.* 9 (2007)
9. K Tsunashima, M Sugiya *Electrochemistry* 75 (2007)
10. L A Aslanov *Ionnye Zhidkosti v Ryadu Rastvoritelei* (Ionic Liquids Among Solvents) (Eds L A Aslanov, M A Zakharov, N L Abramycheva) (Moscow: Moscow State University, 2005)
11. J S Wilkes, M J Zaworodtko *J. Chem. Soc., Chem. Commun.* 965 (1992)
12. M Moreno-Maas, R Pleixats *Acc. Chem. Res.* **36** 638 (2003)
13. M T Reetz, R Breinbauer, K Wanninger *Tetrahedron Lett.* **37** 4499 (1996)
14. R R Deshmukh, R Rajagopal, K V Srinivasan *Chem. Commun.* 1544 (2001)
15. L Xu, W Chen, J Xiao *Organometallics* **19** 1123 (2000)
16. V Calo, A Nacci, A Monopoli, S Laera, N Cioffi *J. Org. Chem.* **68** 2929 (2003)
17. C W Scheeren, G Machado, J Dupont, P F P Fichtner, S R Texeira *Inorg. Chem.* **42** 4738 (2003)
18. D Astruc *Inorg. Chem.* **46** 1884 (2007)
19. D Zhao, Z Fei, T J Geldbach, R Scopelliti, P J Dyson *J. Am. Chem. Soc.* **126** 15876 (2004)
20. F Bernardi, M C M Alves, C W Scheeren, J Dupont, J Morais *J. Electron Spectrosc. Relat. Phenom.* **156–158** 186 (2007)
21. Y-H Zhu, C Koh, T P Ang, A Emi, W Monalisa, L K-J Louis, N S Hosmane, J A Maguire *Inorg. Chem.* **47** 5756 (2008)
22. L S Ott, M L Cline, M Deetlefs, K R Seddon, R G Finke *J. Am. Chem. Soc.* **127** 5758 (2005)
23. G S Fonseca, A P Umpierre, P F P Fichtner, S R Teixera, J Dupont *Chem.–Eur. J.* **9** 3263 (2003)
24. Y-H Zhu, E Widjaja, S Lo Pei Sia, W Zhan, K Carpenter, J A Maguire, N S Hosmane, M F Hawthorne *J. Am. Chem. Soc.* **129** 6507 (2007)
25. M H G Prechtl, M Scariot, J D Scholten, G Machado, S R Teixeira, J Dupont *Inorg. Chem.* **47** 8995 (2008)
26. B Leger, A Denicourt-Nowicki, H Olivier-Bourbigou, A Roucoux *Inorg. Chem.* **47** 9090 (2008)

27. M A Gelesky, A P Umpierre, G Machado, R R B Correia, W C Magno, J Morais, G Ebeling, J Dupont *J. Am. Chem. Soc.* **127** 4588 (2005)
28. F-H Yen, C-C Tai, J-F Huang, I-W Sun *J. Phys. Chem. B* **110** 5215 (2006)
29. E Redel, R Thomann, C Janiak *Inorg. Chem.* **47** 14 (2008)
30. H Zhang, H Cui *Langmuir* **25** 2604 (2009)
31. Y Jin, P Wang, D Yin, JLiu, L Qin, N Yu, G Xie, B Li *Colloid Surf. A* **302** 366 (2007)
32. H Itoh, K Naka, Y Chujo *J. Am. Chem. Soc.* **126** 3026 (2004)
33. J Dupont, G S Fonseca, A P Umpierra, P F P Fichtner *J. Am. Chem. Soc.* **124** 4228 (2002)
34. E T Silveira, A P Umpierre, L M Rossi, G Machado, J Morais, G V Soares, I L R Baumvol, S R Teixeira, P F P Fichtner, J Dupont *Chem. – Eur. J.* **10** 3734 (2004)
35. Y-J Zhu, W-W Wang, R-J Qi, X-L Hu *Angew. Chem., Int. Ed.* **43** 1410 (2004)
36. F Endres, M Bukowski, R Hempelmann, H Natter *Angew. Chem., Int. Ed.* **42** 3428 (2003)
37. A I Bhatt, A Mechler, L L Martin, A M Bond *J. Mater. Chem.* **17** 2241 (2007)
38. H-J Chen, S-J Dong *Langmuir* **23** 12503 (2007)
39. G-T Wei, Z Yang, C-Y Lee, H-Y Yang, C R C Wang *J. Am. Chem. Soc.* **126** 5036 (2004)
40. H S Schrekker, M A Gelesky, M P Stracke, C M L Schrekker, G Machado, S R Teixeira, J C Rubim, J Dupont *J. Colloid Interface Sci.* **316** 189 (2007)
41. K-S Kim, D Demberelnyamba, H Lee *Langmuir* **20** 556 (2004)
42. S Gao, H Zhang, X Wang, W Mai, C Peng, L Ge *Nanotechnology* **16** 1234 (2005)
43. Y Jiang, Y-J Zhu *J. Phys. Chem. B* **109** 4361 (2005)
44. Y Jiang, Y-J Zhu, G-F Cheng *Cryst. Growth Des.* **6** 2174 (2006)
45. Y Che, Q Yang, L Guo, Q Wang, T Ji, Y Deng, in *The 6th International Conference on Materials Processing, Properties and Performance (MP^3-2007), Beijing, China, 2007* p. 25
46. K Yoo, H Choi, D D Dionysiou *Chem. Commun.* 2000 (2004)
47. Y Zhou, M Antonietti *J. Am. Chem. Soc.* **125** 14960 (2003)
48. W Zheng, X Liu, Z Yan, L Zhu *ACS Nano* **3** 115 (2009)
49. I Mukhopadhyay, W Freyland *Langmuir* **19** 1951 (2003)
50. P Wang, S M Zakeeruddin, P Comte, I Exnar, M Grtzel *J. Am. Chem. Soc.* **125** 1166 (2003)
51. L Wang, L Chang, B Zhao, Z-Y Yuan, G-S Shao, W-J Zheng *Inorg. Chem.* **47** 1443 (2008)
52. J Wang, J-M Cao, S-G Deng, H-M Ji, B-Q Fang, H-Y Wang, J Tao, in *Book of Abstracts of the 228th ACS National Meeting, Philadelphia, PA, 2004* p. 562
53. A Thirumurugan, C N R Rao *Cryst. Growth Des.* **8** 1640 (2008)
54. J-M Ma, X Liu, Y Wu, P Peng, W-J Zheng *Cryst. Res. Technol.* **43** 1052 (2008)
55. A Thirumurugan *Bull. Mater. Sci.* **30** 179 (2007)
56. Y Zhou, M Antonietti *Chem. Mater.* **16** 544 (2004)
57. K Ueno, K Hata, T Katakabe, M Kondoh, M Watanabe *J. Phys. Chem. B* **112** 9013 (2008)
58. K Ueno, A Inaba, M Kondoh, M Watanabe *Langmuir* **24** 5253 (2008)
59. S Letaief, T Diaco, W Pell, S I Gorelsky, C Detellier *Chem. Mater.* **20** 7136 (2008)
60. H Zhang, G Chen *Environ. Sci. Technol.* **43** 2905 (2009)
61. B K Price, J L Hudson, J M Tour *J. Am. Chem. Soc.* **127** 14867 (2005)
62. P J Boul, D-G Cho, G M A Rahman, M Marquez, Z-P Ou, K M Kadish, D M Guldi, J L Sessler *J. Am. Chem. Soc.* **129** 5683 (2007)
63. Y-J Zhang, Y-F Shen, J-H Li, L Niu, S Dong, A Ivaska *Langmuir* **21** 4797 (2005)
64. D D Lovingood, G F Strouse *Nano Lett.* **8** 3394 (2008)
65. J Lian, T Kim, X Liu, J Ma, W Zheng *J. Phys. Chem. C* **113** 9135 (2009)
66. S Zein El Abedin, F Endres *Acc. Chem. Res.* **40** 1106 (2007)
67. C Sievers, O Jimenez, T E Müller, S Steuernagel, J A Lercher *J. Am. Chem. Soc.* **128** 13990 (2006)
68. A Narita, K Naka, Y Chujo, in *Ionic Liquid Applications: Pharmaceuticals, Therapeutics and Biotechnology (ACS Symp. Ser.)* Vol. 1038 (Washington, DC: American Chemical Society, 2010) p. 103
69. A Narita, K Suzuki, K Fukumoto, K Naka, H Ohno, Y Chujo, in *Book of Abstract of the EURCHEMConference on Molten Salts and Ionic Liquids, Copenhagen, Denmark, 2008* p. B88
70. N P Tarasova, G V Nad'yarnykh, V V Kostikov, V N Chistyakov, Yu V Smetannikov *Vysokomol. Soedin., Ser. A* **38** 1467 (1996) [a]
71. N P Tarasova, Yu V Smetannikov, I M Artemkina, A S Vilesov, in *Book of Abstracts of the 42nd World Chemistry Congress. Chemistry Protecting Health, Natural Environment and Cultural Heritage, Turin, Italy, 2007* p. 128
72. N P Tarasova, Yu V Smetannikov, I M Artemkina, I A Lavrov, M A Sinaiskii, V I Ermakov *Dokl. Akad. Nauk* **410** 640 (2006) [b]
73. N P Tarasova, Yu V Smetannikov, D E Polyiansky, in *Green Industrial Applications of Ionic Liquids (NATO Sci. Ser. II)* Vol. 92 (Eds R D Rodgers, K R Seddon, S Volkov) (Dordrecht: Kluwer Academic, 2003) p. 537
74. N P Tarasova, Yu V Smetannikov, A S Vilesov, A A Zanin *Pure Appl. Chem.* **81** 2014 (2009)
75. N P Tarasova, Yu V Smetannikov, I M Artemkina, A S Vilesov *Phosphorus, Sulfur Silicon Relat. Elem.* **183** 586 (2008)
76. Y Y He, Z B Li, P Simone, T P Lodge *J. Am. Chem. Soc.* **128** 2745 (2006)
77. M U Araos, G G Warr *J. Phys. Chem. B* **109** 14275 (2005)
78. S-M Yu, F Yan, X-W Zhang, J You, P Wu, J-M Lu, Q-F Xu, X-W Xia, G Ma *Macromolecules* **41** 3389 (2008)
79. N Li, S Zhang, L Zheng, J Wu, X Li, L Yu *J. Phys. Chem. B* **112** 12453 (2008)
80. H Zhang, K Hong, J W Mays *Macromolecules* **35** 5738 (2002)
81. D Wei, C Kvarnstrom, T Lindfors, A Ivaska *Electrochem. Commun.* **8** 1563 (2006)
82. J-Y Kim, J-T Kim, E-A Song, Y-K Min, H-O Hamaguchi *Macromolecules* **41** 2886 (2008)

[a] — *Polym. Sci. (Engl. Transl.)*
[b] — *Dokl. Chem. (Engl. Transl.)*